

Cold exciton gases in coupled quantum well structures

L V Butov

Department of Physics, University of California at San Diego, La Jolla, CA 92093-0319, USA

Received 23 October 2006

Published 11 June 2007

Online at stacks.iop.org/JPhysCM/19/295202

Abstract

Cold exciton gases can be implemented in coupled quantum well structures. In this contribution, we review briefly the recent works on spontaneous coherence of cold excitons and on trapping of cold excitons with laser light.

(Some figures in this article are in colour only in the electronic version)

1. Introduction

1.1. The exciton condensates

Electron–hole systems in semiconductors provide an opportunity for studying a rich variety of collective states. The first example is an electron–hole droplet. It is a condensate in real space of degenerate electron and hole Fermi liquids. A review of electron–hole droplets can be found in [1], and for recent advances in the field see [2].

It was also shown that bound electron–hole pairs—excitons—are hydrogen-like bosons at low densities $na_B^D \ll 1$ [3] and Cooper-pair-like bosons at high densities $na_B^D \gg 1$ [4] (a_B is the exciton Bohr radius, n the density, and D the dimensionality). The bosonic nature of excitons makes possible their condensation in momentum space, i.e. high occupation of a state with the occupation number $N_p \gg 1$. Designing semiconductor structures with the required characteristics and varying the exciton density, photon numbers, and other parameters allows an experimental probe of the various types of exciton condensate in momentum space.

The first type of exciton condensate is the condensate of polaritons, which is implemented in semiconductor microcavities. This condensate is characterized by substantial coupling of excitons to the optical field, a short lifetime of the polaritons, of the order of a few picoseconds, and a small polariton mass, $\sim 10^{-4} m_0$ (m_0 is the free electron mass) [5]. According to the theory [6], coherence in the polariton system forms due to a macroscopic coherent optical field similar to coherence in lasers. (The relation between coherence and condensation is discussed in section 2.) The polariton condensates, also called polariton lasers [7], have attracted considerable interest over the last decade. Recent advances in their studies, which are reported for instance in [8–10], are reviewed in other contributions to this issue.

The second type of exciton condensate is the BCS-like condensate, also called the excitonic insulator [4]. For this condensate, electrons and holes are (nearly) uncorrelated above the critical temperature and the pairs—excitons—are formed below the critical temperature. Implementation of the excitonic insulators in photoexcited semiconductor systems is

challenging mainly due to the problem of cooling the high-density photoexcited electron–hole plasmas below the critical temperature. An alternative approach is based on equilibrium semimetal-like electron–hole systems [11]. Such systems can be implemented in semiconductor quantum well (QW) structures [12]. In both the semimetal and semiconductor systems the interband transitions, which are generally referred to as electron–hole recombination for semiconductors and tunnelling for semimetals, destroy the coherent properties of the condensate [13, 14]. However, those transitions can be made negligibly small by spatial separation between the electron and hole layers in coupled quantum well (CQW) structures [15].

A new collective state has been discovered recently in two-dimensional electron gas (2DEG) bilayers in high magnetic fields at the filling factor $\nu = 1$ [16–20]. This state was elegantly interpreted in terms of excitons [21]. The correlated electron–hole pairs in 2DEG bilayers—magnetoexcitons—are formed below the critical temperature, and therefore this collective state has similarities with the BCS-like exciton condensate.

The third type of exciton condensate is the BEC-like condensate, which forms in a gas of (weakly) interacting hydrogen-like excitons at low densities $na_B^D \ll 1$ [3]. In contrast to the BCS-like condensate, in the case of an exciton BEC the excitons are not created at the critical temperature and instead condense to the lowest energy state due to the thermal distribution. In contrast to the polariton lasers, in the case of an exciton BEC, coupling of excitons to the optical field is not essential for establishing coherence. In turn, the critical temperature of this type of exciton condensate is given by the critical temperature for the BEC and the analogy extends to other condensate properties [3]. We note parenthetically that the repulsive interaction leads to the enhancement of the critical temperature [3, 22].

According to the theory, the transition between the different types of exciton condensate can be implemented by varying the parameters. For instance, the transition from BEC to BCS condensates in a system of photoexcited excitons can occur with increasing density [4, 23], while the transition from BEC or BCS to laser can occur with increasing coupling of excitons to photons and photon numbers [6].

In this contribution, we review briefly the studies of a system of cold hydrogen-like low-density excitons. The exciton condensation in such systems corresponds to the exciton BEC.

The excitons have finite lifetimes, and their temperature is determined by the ratio of the exciton energy relaxation and recombination rates. Therefore experimental implementation of cold exciton gases requires systems with long exciton lifetimes and fast cooling.

Over the last two decades the experimental efforts to implement cold exciton gases in bulk semiconductors, ultimately with temperatures below the critical temperature for a BEC, dealt mainly with bulk Cu_2O [24–28], a material whose ground exciton state is optically dipole inactive and which has, therefore, a low radiative recombination rate. Recent measurements indicate that the exciton densities reached in recent experiments in Cu_2O until now are far below that required to achieve the exciton BEC, presumably due to the high Auger recombination rate in Cu_2O [29–33], and the phenomena observed in Cu_2O , while being interesting by themselves, are explained within a classical framework not related to BEC [29–36].

In order to create cold exciton gases we work with CQW structures. In CQWs, the exciton lifetime is long due to the spatial separation between electrons and holes, which are confined in different QWs (figure 2(a)) [15, 37]: in the CQW samples that we study the lifetime of the indirect excitons is controlled *in situ* by gate electrodes typically in the range from a few tens of nanoseconds to a few microseconds, thus being from three (four) to five (six) orders of magnitude longer than the lifetime of the regular direct excitons (microcavity polaritons); for a review see [38] (in GaAs single QWs, the exciton lifetime is 20 ps [39, 40]). Besides, the cooling of hot photoexcited excitons down to the temperatures of the cold lattice, which occurs via emission of bulk LA phonons, is about three orders of magnitude faster for excitons in QWs

than that in the bulk material. This is due to relaxation of the momentum conservation law in the direction perpendicular to the QW plane. Indeed, for quasi-2D systems the ground-state mode $E = 0$ couples to the continuum of the energy states $E \geq E_0$ rather than to the single energy state $E = E_0 = 2 M v_s^2$ (v_s is the velocity of sound) as occurs in bulk semiconductors [41, 42].

Because of the long lifetime and high cooling rate, indirect excitons form a unique system where cold exciton gases with temperatures well below 1 K can be formed. The calculations of the exciton kinetics [43] show that a gas of indirect excitons in the CQW cools down to 100 mK in about 70 ns after switching off the excitation pulse, and the accuracy of the calculations is confirmed by the quantitative agreement with experiment [43]. Since the lifetime of the indirect excitons can be significantly longer than 70 ns, a dense and cold gas of indirect excitons with temperatures lower than 100 mK and density in excess of 10^{10} cm^{-2} is implemented in dilution refrigerators with low bath temperature $T_b \lesssim 50 \text{ mK}$ [38]. The estimates below show that an exciton gas with these parameters is ultracold. Therefore CQWs allow creating and studying ultracold exciton gases.

Note that in real CQW samples the leakage current due to the photoexcitation and applied voltage can in principle lead to extrinsic, i.e. not by design, heating of excitons. For instance, the authors of [46] show that the indirect excitons in their samples do not cool below about 5 K, presumably due to the high leakage current. In order to implement cold exciton gases in CQW structures, all extrinsic heating sources, such as leakage current, nonradiative recombination, and others, must be suppressed. The quantitative agreement between the calculations and experiments [43–45] proves the absence of noticeable extrinsic heating in the CQW samples studied in [43–45, 47–49, 55, 62, 65, 71].

Below we estimate how cold the exciton gas in CQWs should be to achieve quantum degeneracy. The transition from a classical to a quantum gas occurs when bosons are cooled to the point where the thermal de Broglie wavelength $\lambda_{dB} = \sqrt{2\pi\hbar^2/(mk_B T)}$ is comparable to the interparticle separation (for instance, BEC takes place when $n\lambda_{dB}^3 = 2.612$ in 3D systems) and the transition temperature for excitons in GaAs/AlGaAs QWs reaches a value of $T_{dB} = 2\pi\hbar^2 n/(mgk_B) \approx 3 \text{ K}$ for the exciton density per spin state $n/g = 10^{10} \text{ cm}^{-2}$ (the exciton spin degeneracy $g = 4$ and the exciton mass $m = 0.22m_0$ for GaAs/AlGaAs QWs [47–49]). Note that at this density $na_B^2 \sim 0.1$ and, therefore, excitons are interacting hydrogen-like Bose particles [3] ($a_B \approx 20 \text{ nm}$ is the exciton Bohr radius [50]).

It is also essential that the indirect excitons in CQWs are dipoles oriented perpendicular to the QW plane. The repulsive interaction between such dipoles stabilizes the exciton state against the formation of metallic electron–hole droplets [51, 52]. Besides, repulsive interaction results in screening of in-plane disorder potential [53] and therefore improves the sample quality. In experiments, the repulsive interaction is revealed by the enhancement of the exciton energy with increasing density [54, 55]. The density of the indirect excitons can be estimated with high accuracy from this energy shift, $n = \varepsilon_b \delta E / (4\pi e^2 d)$ [56] (d is the separation between the electron and hole layers and ε_b is the background dielectric constant).

In earlier studies, the formation of cold exciton gases in CQWs was demonstrated, and evidence for a set of phenomena expected for exciton condensation was observed in cold exciton gases: a strong enhancement of the indirect exciton mobility, which is consistent with the onset of exciton superfluidity [57]; a strong enhancement of the exciton radiative decay rate, which is consistent with exciton condensate superradiance [57]; fluctuations of the indirect exciton emission, which are suggestive of fluctuations near the phase transition [54]; a strong enhancement of the exciton scattering rate with increasing exciton concentration revealing bosonic stimulation of exciton scattering [43]; and narrowing of the exciton PL spectra, which is consistent with narrowing of the exciton energy distribution [58, 60, 61]. While all these phenomena are observed at expected parameters for the exciton BEC (below the estimated

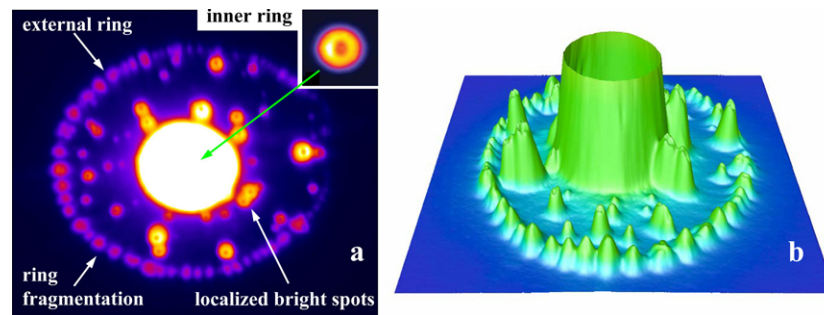


Figure 1. (a) 2D and (b) 3D images of the spatial PL pattern in a CQW structure. The pattern features include the inner exciton ring, the external exciton ring, the localized bright spots (LBSs), and the macroscopically ordered exciton state (MOES)—a periodic array of beads with spatial order on a macroscopic length. The MOES forms in the external ring at low temperatures below a few kelvin. From [65] and [44].

BEC critical temperature), are consistent with the expected specific properties of the exciton BEC, and have no alternative to BEC explanation so far, they do not present unambiguous evidence for the exciton BEC. (Regarding the absence of alternative explanations, it should be noted that one of these phenomena, namely narrowing of the exciton PL spectra [58, 60, 61], was also discussed in terms of the exciton redistribution in the in-plane random potential [59].)

1.2. The exciton pattern formation

Recently, spatial photoluminescence (PL) patterns have been observed in structures with coupled [62–65] and single [66] quantum wells. The pattern features include the inner exciton rings [62], the external exciton rings [62–66], the localized bright spots (LBSs) [62, 65, 67, 68], and the macroscopically ordered exciton state (MOES)—a periodic array of beads with spatial order on a macroscopic length (figure 1) [62, 65].

The inner and outer exciton rings and LBSs are observed up to high temperatures and are classical phenomena. Their origin has been identified: the inner ring has been explained in terms of nonradiative exciton transport and cooling [44] and the external rings and LBSs have been explained in terms of macroscopic in-plane charge separation and exciton formation at the interface of the electron- and hole-rich regions [65, 66]. We stress that bringing the external ring as evidence of a BEC and superfluidity by Snoke in [63, 64] is inconsistent since the ring is observed up to high temperatures, which exceed T_{dB} by more than order of magnitude and even substantially exceed the exciton binding energy [50, 69]. The later fact means that the external ring is observed even at temperatures where overwhelming majority of excitons dissociate according to the Saha equation [70].

In contrast, the MOES is a low-temperature phenomenon. The MOES appears abruptly in the external rings at low temperatures below a few kelvin [62, 65]. Research to understand the origin of the MOES is in progress.

2. Spontaneous coherence of cold excitons

In this section, we briefly review the recent work on spontaneous coherence of cold excitons [71].

Coherence of excitons in quantum wells attracts considerable interest. It has been intensively studied by four-wave mixing [72], coherent control [73], and interferometric and

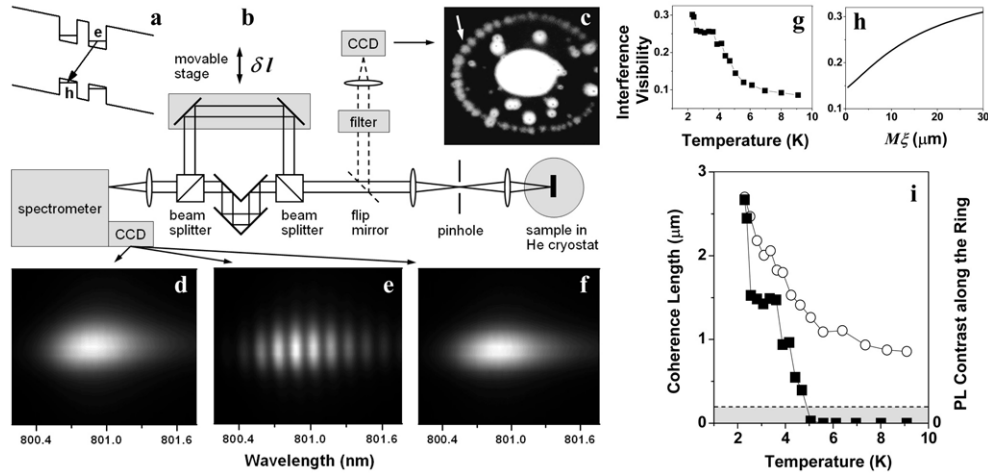


Figure 2. (a) The CQW band diagram. (b) Scheme of MZ interferometer with spatial and spectral resolution. (c) The pattern of indirect exciton PL. The area of view is $280 \mu\text{m} \times 250 \mu\text{m}$. Spectra for the left (d), right (f), and both (e) arms of the MZ interferometer. The light was selected from the centre of the arrow-marked MOES bead. The length of view (vertical axis) is $25 \mu\text{m}$. (g) Visibility of the interference fringes versus T . (h) Calculated visibility as a function of the coherence length for $M_2 = 1.7$. (i) The exciton coherence length (squares) and contrast of the spatial intensity modulation along the ring (circles) versus T . The shaded area is beyond experimental accuracy. $V_g = 1.24 \text{ V}$, $P_{\text{ex}} = 0.7 \text{ mW}$, and $\delta l = 4.2 \text{ mm}$ for all the data. $T = 1.6 \text{ K}$ for the data in (c)–(f). $D = 25 \mu\text{m}$, for the data in (d)–(f) and $50 \mu\text{m}$ for the data in (g), (h). From [71].

speckle analysis of resonant Rayleigh scattering [74–76]. In all these experiments, exciton coherence was induced by a resonant laser excitation and was lost within a few picoseconds after the excitation pulse due to exciton–exciton and exciton–phonon collisions and due to inhomogeneous broadening by disorder.

Another fundamentally interesting type of coherence is spontaneous coherence (not driven by the laser excitation). It is related to the exciton momentum distribution. For free particles the coherence length ξ and the spread of the momentum distribution δk are related by $\xi \delta k \sim \pi$, see e.g. [77]. For a classical thermal gas the coherence length is given by the de Broglie wavelength, $\sim 0.1 \mu\text{m}$ at $T = 2 \text{ K}$, while for a condensate with narrow momentum distribution the coherence length exceeds this value and ultimately reaches the size of the system.

Spontaneous coherence can be experimentally studied using nonresonant laser excitation so that the coherence is not driven by the laser. However, nonresonant excitation may lead to strong heating of the excitons in the excitation spot [43–45]. Therefore, here we review studies of coherence in the external exciton rings [62], which form far away from the excitation spot (figure 1), at the border between the electron- and hole-rich regions [65, 66]. The external ring of indirect excitons in CQWs is the region where the exciton gas is cold: the excitons in the ring are formed from well-thermalized carriers and their temperature essentially reaches that of the lattice. The cold exciton gas in the external ring can form the MOES [62]. The MOES appears abruptly along the ring at T below a few kelvin.

In [71] we reported on the emergence of spontaneous coherence of excitons at low temperatures. The exciton coherence length increases strongly below a few kelvin, in concert with the macroscopic spatial ordering of excitons. At the lowest T the measured coherence length corresponds to a very narrow spread of exciton momentum distribution, much smaller than that for a classical exciton gas.

Spontaneous coherence of excitons translates into coherence of the emitted light [78–81]. To probe it several optical experimental techniques have been proposed: a second-order optical response [78], Hanbury–Brown–Twiss interferometry [79, 80], and a speckle analysis at off-resonant excitation [81]. Our technique is based on measuring the first-order coherence function of the electric field $E(t, \mathbf{r})$ of the light emitted by excitons. This quantity is defined by [82, 83]

$$g(t, \mathbf{r}) = \langle E(t' + t, \mathbf{r}' + \mathbf{r})E(t', \mathbf{r}') \rangle / \langle E^2(t', \mathbf{r}') \rangle \quad (1)$$

(local ergodicity in space and time is assumed). The linear technique allows us to work with the low-level optical signals of the spatially resolved PL.

Our experimental setup (figure 2(b)) is a variant of Mach–Zehnder (MZ) interferometry with new ingredients. First, we added spatial resolution by collecting the light only from a selected area of size $D/M_1 = 2\text{--}10 \mu\text{m}$ in the middle of an MOES bead (figure 2(c)). This was done by placing a pinhole of diameter $D = 10\text{--}50 \mu\text{m}$ at the intermediate image plane of magnification $M_1 = 5$. Second, we added the frequency resolution by dispersing the output of the MZ interferometer with a grating spectrometer. (The image was further magnified by the factor $M_2 \approx 2$ after the pinhole.) The output of the spectrometer was imaged by a nitrogen-cooled CCD (figure 2(b)). The MZ delay length δl was controlled by a piezo-mechanical translation stage. The PL pattern of the indirect excitons (figure 2(c)) was also imaged with the pinhole removed and the image filtered at the indirect exciton energy (dashed path in figure 2(b)). The excitation was supplied by a HeNe laser at 633 nm (the laser excitation spot with FWHM $7 \mu\text{m}$ is in the centre of the exciton ring; see figure 2(c)). The excitation was 400 meV above the indirect exciton energy and well separated in space; therefore, no laser-driven coherence was possible in the experiment. The CQW structure with two 8 nm GaAs QWs separated by a 4 nm $\text{Al}_{0.33}\text{Ga}_{0.67}\text{As}$ barrier was grown by molecular-beam epitaxy (MBE); see figure 2(a). For an applied external gate voltage $V_g \approx 1.2 \text{ V}$ the ground state is an indirect exciton with a lifetime $\tau_{\text{rec}} \sim 40 \text{ ns}$ (details of the CQW structures can be found in [38]).

An example of the measured interference pattern is shown in figure 2(e). The light was collected from the centre of the bead shown in figure 2(c) by the arrow. The modulation period $\delta\lambda$ of the CCD signal I was found to obey the expected dependence $\delta\lambda = \lambda^2/\delta l$. To quantify the amplitude of the modulations we computed their visibility factor $V = (I_{\text{max}} - I_{\text{min}})/(I_{\text{max}} + I_{\text{min}})$ using a method based on Fourier analysis. The visibility factor was examined for a set of δl and T . The details of the method are described in [71].

The main experimental result is presented in figure 2(g): visibility of the interference fringes sharply increases at temperatures below a few kelvin. This contrasts with the T -independent V of the direct exciton emission measured at the excitation spot centre at $T = 2\text{--}10 \text{ K}$.

The theoretical data analysis is described in [71]. By analogy to the first-order coherence function (equation (1)) at the coincident points for a classical source with a Lorentzian emission lineshape $g(t, \mathbf{r} = 0) = \exp(-t/\tau_c)$, where τ_c is the inverse linewidth, we assume the r -dependence in the form $g(t, \mathbf{r}) = g(t, 0) \exp(-r/\xi)$, where ξ is the coherence length. We deduce ξ from the contrast of the periodic modulations in the CCD image, figure 2(e), as described in [71]. The measured $V(T)$, figure 2(g), and the calculated $V(\xi)$, figure 2(h), allow us to obtain the coherence length $\xi(T)$. Figure 2(i) shows that the coherence length increases sharply at T below a few kelvin. Intriguingly, the increase of ξ is in concert with the MOES formation.

Naively, the interference pattern of an extended source of length ξ washes out when $\xi \delta k \sim \pi$, where δk is the spread of the momentum distribution. For $\xi \sim 2 \mu\text{m}$ (figure 2(i)),

this gives $\delta k \sim 10^4 \text{ cm}^{-1}$, which is much smaller than the spread of the exciton momentum distribution in a classical exciton gas $\delta k_{\text{cl}} \sim \hbar^{-1} \sqrt{2mk_{\text{B}}T} \approx 3 \times 10^5 \text{ cm}^{-1}$ at $T = 2 \text{ K}$. In turn, this corresponds to a spread of the exciton energy distribution $\hbar^2 \delta k^2 / 2m \sim 1 \text{ } \mu\text{eV}$, which is much smaller than that for a classical exciton gas $\delta E_{\text{cl}} \sim k_{\text{B}}T \approx 200 \text{ } \mu\text{eV}$ at $T = 2 \text{ K}$. The coherence length $\xi \sim 2 \text{ } \mu\text{m}$ strongly exceeds the classical value, which is given by the de Broglie wavelength, $\sim 0.1 \text{ } \mu\text{m}$ at $T = 2 \text{ K}$. It may also be interesting to estimate the exciton phase-breaking time $\tau_{\phi} = \xi^2 / D_x$, where $D_x \sim 10 \text{ cm}^2 \text{ s}^{-1}$ [44] is the exciton diffusion coefficient. Using again $\xi = 2 \text{ } \mu\text{m}$, we get τ_{ϕ} of a few nanoseconds. In comparison, the inverse linewidth $\tau_c \approx 1 \text{ ps}$.

Let us now discuss physical mechanisms that may limit ξ and τ_{ϕ} . Since $\tau_{\text{rec}} \sim 40 \text{ ns} \gg \tau_{\phi}$, the effect of exciton recombination on the phase-breaking time is negligible. Next, the excitons are highly mobile, as evidenced by their large diffusion length, about $30 \text{ } \mu\text{m}$ [84]; therefore, ξ is not limited by disorder localization. The coherence length may also be limited by inelastic collisions of excitons with phonons and with each other. For the high exciton densities $n \sim 10^{10} \text{ cm}^{-2}$ in our experiments, the dominant ones are the latter [42]. Note also that the spontaneous coherence we report arises in a cold thermalized exciton gas (the lifetime τ_{rec} of the indirect excitons is much longer than their thermalization time to $T = 2 \text{ K}$, $\sim 1 \text{ ns}$ [43]).

Note also that the system of indirect excitons is characterized by design by negligibly small coupling of excitons to photons. Therefore, spontaneous coherence emerging in the system of cold indirect excitons is similar to coherence in ultracold matter and is different from the laser-like coherence due to a macroscopic coherent optical field. The latter type of coherence is characteristic for systems like microcavity polariton lasers, where coupling to the optical field is essential for establishing coherence [6].

Theoretical calculation of ξ due to exciton interactions is yet unavailable. It is expected, however, that inelastic processes should vanish at $T = 0$. Our findings call for developing a quantitative theory of phase-breaking processes in nonclassical exciton gases at low temperatures when the thermal de Broglie wavelength is comparable to the interparticle separation.

3. Trapping of cold excitons with laser light

In this section, we briefly review the idea of trapping of cold excitons with laser light and its experimental implementation [45].

Lasers enable a precise and non-invasive application of force while also providing high-speed control of the trapping field. This allows *in situ* trapping and control for a rich variety of small neutral particles. Since their invention three decades ago, laser-based traps have been key devices in the advancement of atomic physics and biophysics; for reviews see [85–88].

In atomic physics, the use of the Doppler cooling technique [89] by sets of counter-propagating lasers is employed to form an ‘optical molasses’ containing atoms viscously confined at microkelvin temperatures. The introduction of optical tweezers to this molasses enabled the first 3D stable trap for atoms by capturing them from the surrounding molasses. Following this initial trapping of atoms, much work was devoted to the creation of larger-volume magneto-optical traps (MOTs) to enhance the achievable densities of trapped atoms [85–88]. It was specifically these MOTs that led to the first realizations of BEC in atoms [90–92]. Since this initial realization of BEC, interest has returned again to optical traps, which can be used to study magnetic effects on BEC, such as Feshbach resonances, without the complexity added by disrupting the magnetic field used in MOTs [85–88]. The possibility of patterning and controlling the potential profile by laser excitation is also effectively employed in studies of atom BEC in optical lattices [93].

Recently [45], we proposed and demonstrated laser-induced trapping for a new system—a gas of excitons in CQWs. Since the quantum degeneracy temperature scales inversely with the mass, quantum exciton gases can be achieved at temperatures of a few kelvin [3], see above, several orders of magnitude higher than quantum atom gases [94, 95]. Therefore, we chose indirect excitons for development of a method to trap cold excitons with laser light. This technique opens a pathway towards high-speed control of quantum gases of bosons in semiconductors—quantum exciton gases.

The possibility of exciton confinement and manipulation in potential traps attracted considerable interest in earlier studies. Pioneered by the electron–hole liquid confinement in the strain-induced traps [96], exciton confinement has been implemented in various traps: strain-induced traps [97, 98], traps created by laser-induced local interdiffusion [99], magnetic traps [100], and electrostatic traps [101–103].

The principle underlying the new method of laser-induced exciton trapping is described below. The CQW geometry [38] is engineered so that the interaction between excitons is repulsive: indirect excitons, formed from electrons and holes that are confined to different QWs by a potential barrier, behave as dipoles oriented perpendicular to the plane, and an increasing exciton density causes an increase of the interaction energy [51–53]. The repulsive character of the interaction is evidenced in experiments as a positive and monotonic line shift with increasing density [54, 55]. Due to the repulsive interaction, a ring-shaped laser spot should form a potential trap with the energy minimum at the ring centre. Similarly to all optical traps, an important advantage of laser-induced exciton trapping is the possibility of controlling the trap *in situ* by varying the laser intensity in space and time. Moreover, the excitons at the trap centre are cold since they are far from the hot laser excitation ring. The long lifetimes of the indirect excitons allow them to travel to the trap centre, due to their drift and diffusion, before optical recombination. This leads to accumulation of a cold and dense exciton gas at the trap centre. The implementation of this idea is briefly described below.

In our experiments, the spatial x – y PL pattern is acquired by a nitrogen-cooled CCD camera after spectral selection by an interference filter chosen to match the indirect exciton energy exclusively. As a result, we are able to remove the low-energy bulk emission that otherwise dominates the spectrum under the laser excitation area. This allows the direct visualization of the indirect exciton PL emission intensity profile in spatial coordinates (see figures 3(b)–(d)). In addition, in figure 3(a) we plot the exciton PL in the *energy–coordinate* plane as measured when a slit along the diameter of the ring is dispersed by a spectrometer without spectral selection by an interference filter. Our investigations determined that a laser excitation ring with a diameter of $30\ \mu\text{m}$ and a ring thickness following a Gaussian profile of $\text{FWHM} = 2\sigma \simeq 7\ \mu\text{m}$ provided the optimal conditions for our CQW sample. The ring-shaped cw laser excitation was performed by a Nd:YVO₄ laser at 532 nm, or HeNe laser at 633 nm, or Ti:sapphire laser tuned to the direct exciton resonance of 788 nm. Spatial and spectral features were essentially similar for all excitation wavelengths investigated. In the experiments with excitation above the AlGaAs barrier ($\lambda = 532$ or 633 nm), photoexcited unbalanced charges and the external ring are created, while in the experiments at nearly resonant excitation ($\lambda = 788$ nm), no photoexcited unbalanced charges or external ring are created [65]. Comparison of these two experiments has shown that the charge imbalance and external ring make no noticeable effect on the exciton trapping. All experimental data presented here are from a set of 532 nm excitation ring data taken with excitation powers P_{ex} in the range 1–1000 μW and with gate voltage $V_g = 1.4$ V. The same CQW structure was studied as in the experiment on spontaneous coherence; see above.

As can be seen in figures 3(b)–(d) and 4(a), for low excitation powers the PL profile follows the laser excitation ring; however, with increasing excitation power a spatial PL peak emerges

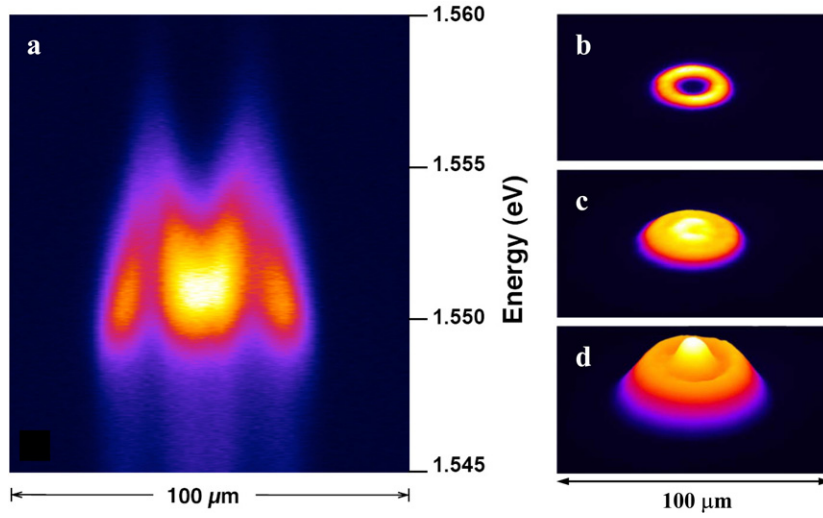


Figure 3. Images of laser-induced trapping of excitons. (a) Image of the PL signal in E - x coordinates. (b)–(d) x - y plots of the PL intensity from indirect excitons created by 532 nm cw laser excitation in a 30 μm diameter ring on the CQW sample. For (b)–(d) the excitation powers are $P_{\text{ex}} = 10, 35, 100 \mu\text{W}$ and for (a) $P_{\text{ex}} = 75 \mu\text{W}$. Sample temperature $T_b = 1.4$ K. From [45].

at the centre of the laser excitation ring, indicating the accumulation of a cold and dense exciton gas. The exciton degeneracy at the trap centre $N_{E=0} = \exp(T_{\text{dB}}/T) - 1$ [42] can be estimated from the exciton density and temperature. The exciton density $n = \epsilon_b \delta E / (4\pi e^2 d)$ is measured directly by the exciton energy shift δE ; see above ($n = 10^{10} \text{ cm}^{-2}$ for $\delta E \simeq 1.6 \text{ meV}$). The exciton temperature at the trap centre is essentially equal to the lattice temperature due to the absence of heating sources at the trap centre. The estimate shows that for the excitation $P_{\text{ex}} = 1 \text{ mW}$ and temperature $T_b = 1.4 \text{ K}$, see the experimental data in figures 3 and 4, the exciton degeneracy at the trap centre is $N_{E=0} \simeq 8$. The theoretical modelling confirms this estimate; see figure 4(f).

Note that the exciton trapping by laser light is based on a different physical principle compared to the atom trapping by laser light. However, the two techniques lead to conceptually similar optical trapping of quantum gases—of excitons or atoms, respectively.

A parabolic energy trap is apparent in the interior of the excitation ring (figures 3(a) and 4(c)). The decrease in the indirect exciton PL at the location of the excitation ring (figure 4(a)) is because the high-energy photogenerated excitons heat the exciton gas; this heating reduces the fraction of optically active excitons, which have low energies, $E \leq E_\gamma = E_g^2 \epsilon_b / (2mc^2)$, where E_g is the energy gap and c is the speed of light [39]. As they drift and diffuse away from the excitation area, the excitons thermalize to the lattice temperature T_b and become optically active, leading to the moderately enhanced PL intensity directly external to the excitation ring. The strong enhancement of the PL at the excitation ring centre, figure 4(a), is due to (1) the excitons' thermalization to the lattice temperature and (2) the accumulation of large numbers of excitons driven by dipole repulsion away from the higher-density region towards the ring centre.

A particular feature of the trap is that it is formed by the indirect excitons themselves: the trap potential is given in the mean-field approximation by $U_{\text{trap}} = \delta E = u_0 n = 4\pi e^2 n d / \epsilon_b$, where u_0 is a positive scattering amplitude. Note that the trap-confining potential is determined

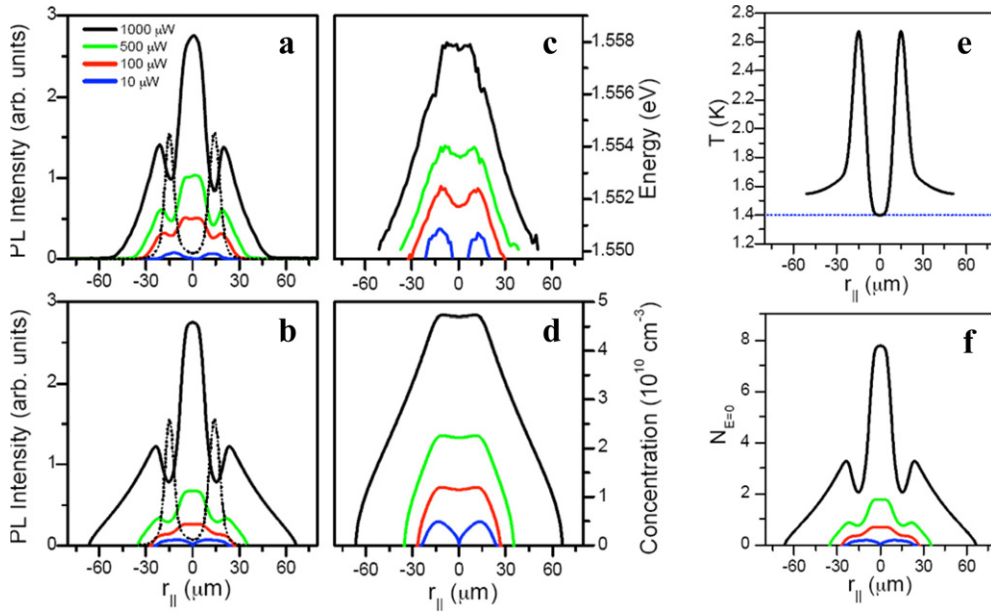


Figure 4. Spatial profiles of the PL intensity and energy for the excitons in the laser-induced trap. (a) Measured PL intensity, (b) calculated PL intensity, (c) measured energy position of the PL line, and (d) calculated exciton concentration against radius $r_{||}$ for four optical excitation powers P_{ex} . The vertical axes of (c) and (d) cover the same range due to the relation $\delta E = 4\pi e^2 n d / \epsilon_b$, where $d = 12$ nm for our sample. The ring-shaped profile of the laser excitation is shown by the thin dotted lines in (a) and (b). Sample temperature $T_b = 1.4$ K. (e) The calculated radial dependence of the exciton temperature T for optical excitation power of $1000 \mu\text{W}$ (solid black) and the lattice temperature $T_b = 1.4$ K (dotted blue). (f) The calculated occupation number $N_{E=0}$ for our samples against radius $r_{||}$ for the same four optical excitation powers as in (a)–(d). From [45].

by the radial exciton density distribution and is essentially independent of other characteristics of indirect excitons such as their temperature, etc.

Accumulation and thermalization of the particles in the laser-induced trap was modelled by solving numerically three coupled nonlinear equations which describe the transport [53], relaxation and PL dynamics [42] of indirect excitons, respectively. The theoretical model is described in [45]. The parameters in the model, such as the diffusion coefficient $D_x^{(2d)}$ and the amplitude of the disorder potential U_{rand} in the CQW structure, were evaluated in the earlier study [44] of the inner PL ring from indirect excitons generated by a point-focused laser beam. The numerical calculations [45] excellently match the experimental results (figures 4(b) and (d)).

The increase of the exciton gas temperature due to heating by photogenerated excitons at the excitation ring is evident in figure 4(e). A minor heating due to the exciton potential energy gradient [45] can also be seen outside the excitation ring. Finally, the theoretical calculations confirm that, in our experiments, which deal with the cryostat temperature $T_b = 1.4$ K, high nonclassical occupation numbers, $N_{E=0} \simeq 8$, build up at the trap centre (figure 4(f)).

4. Summary

In this contribution we have briefly reviewed the studies of various types of exciton condensate as well as the recent works on spontaneous coherence of cold excitons and on trapping of cold excitons with laser light.

A Mach–Zehnder interferometer with spatial and spectral resolution was used to probe the spontaneous coherence in cold exciton gases, which are implemented experimentally in the ring of indirect excitons in coupled quantum wells [71]. A strong enhancement of the exciton coherence length is observed at temperatures below a few kelvin. The increase of the coherence length is correlated with the macroscopic spatial ordering of excitons. The coherence length at the lowest temperature corresponds to a very narrow spread of the exciton momentum distribution, much smaller than that for a classical exciton gas.

We proposed laser-induced trapping for a gas of excitons in quantum well structures and demonstrated the trapping of a highly degenerate Bose gas of excitons in laser-induced traps [45]. An important advantage of laser-induced exciton trapping is the possibility of high-speed control of degenerate exciton gases in the traps *in situ* by varying the laser intensity in space and time.

Acknowledgments

The works on spontaneous coherence of cold excitons and on trapping of cold excitons with laser light, which are reviewed in this contribution, were performed in collaboration with M M Fogler, A C Gossard, M Griswold, A T Hammack, A L Ivanov, L E Smallwood, and Sen Yang. This work is supported by NSF grant DMR-0606543 and ARO grant W911NF-05-1-0527. We thank K L Campman for growing the high-quality samples, and M Hanson, J Keeling, L V Keldysh, L S Levitov, L J Sham, B D Simons, D E Smith, and A V Sokolov for discussions.

References

- [1] Keldysh L V 1986 *Contemp. Phys.* **27** 395
- [2] Jiang J H, Wu M W, Nagai M and Kuwata-Gonokami M 2005 *Phys. Rev. B* **71** 035215
- [3] Keldysh L V and Kozlov A N 1968 *Zh. Eksp. Teor. Fiz.* **54** 978
Keldysh L V and Kozlov A N 1968 *Sov. Phys.—JETP* **27** 521 (Engl. Transl.)
- [4] Keldysh L V and Kopaev Yu V 1964 *Fiz. Tverd. Tela* **6** 2791
Keldysh L V and Kopaev Yu V 1965 *Sov. Phys.—Solid State* **6** 2219 (Engl. Transl.)
- [5] Weisbuch C, Nishioka M, Ishikawa A and Arakawa Y 1992 *Phys. Rev. Lett.* **69** 3314
- [6] Littlewood P B, Eastham P R, Keeling J M J, Marchetti F M, Simons B D and Szymanska M H 2004 *J. Phys.: Condens. Matter* **16** S3597
- [7] Imamoglu A and Ram R J 1996 *Phys. Lett. A* **214** 193
- [8] Krizhanovskii D N, Sanvitto D, Love A P D, Skolnick M S, Whittaker D M and Roberts J S 2006 *Phys. Rev. Lett.* **97** 097402
- [9] Kasprzak J, Richard M, Kundermann S, Baas A, Jeambrun P, Keeling J M J, Marchetti F M, Szymanska M H, Andre R, Staehli J L, Savona V, Littlewood P B, Deveaud B and Dang L S 2006 *Nature* **443** 409
- [10] Deng H, Press D, Gotzinger S, Solomon G S, Hey R, Ploog K H and Yamamoto Y 2006 *Phys. Rev. Lett.* **97** 146402
- [11] Halperin B I and Rice T M 1968 *Rev. Mod. Phys.* **40** 755
- [12] Zhu X D, Quinn J J and Gumbs G 1990 *Solid State Commun.* **75** 595
- [13] Kohn W and Sherrington D 1970 *Rev. Mod. Phys.* **42** 1
- [14] Guseinov R R and Keldysh L V 1972 *Zh. Eksp. Teor. Fiz.* **63** 2255
- [15] Lozovik Y E and Yudson V I 1976 *Zh. Eksp. Teor. Fiz.* **71** 738
- [16] Eisenstein J P, Boebinger G S, Pfeiffer L N, West K W and He S 1992 *Phys. Rev. Lett.* **68** 1383
- [17] Lay T S, Suen Y W, Manoharan H C, Ying X, Santos M B and Shayegan M 1994 *Phys. Rev. B* **50** 17725
- [18] Spielman I B, Eisenstein J P, Pfeiffer L N and West K W 2000 *Phys. Rev. Lett.* **84** 5808
- [19] Kellogg M M, Eisenstein J P, Pfeiffer L N and West K W 2004 *Phys. Rev. Lett.* **93** 036801
- [20] Tutuc E, Shayegan M and Huse D A 2004 *Phys. Rev. Lett.* **93** 036802
- [21] Eisenstein J P and MacDonald A H 2004 *Nature* **432** 691
- [22] Leggett A J 2001 *Rev. Mod. Phys.* **73** 307

- [23] Comte C and Nozieres P 1982 *J. Physique* **43** 1069
- [24] Hulin D, Mysyrowicz A and la Guillaume C B 1980 *Phys. Rev. Lett.* **45** 1970
- [25] Snoke D W, Wolfe J P and Mysyrowicz A 1990 *Phys. Rev. Lett.* **64** 2543
- [26] Fortin E, Fafard S and Mysyrowicz A 1993 *Phys. Rev. Lett.* **70** 3951
- [27] Lin J L and Wolfe J P 1993 *Phys. Rev. Lett.* **71** 1222
- [28] Mysyrowicz A, Benson E and Fortin E 1996 *Phys. Rev. Lett.* **77** 896
- [29] O'Hara K E, Suilleabhain L O and Wolfe J P 1999 *Phys. Rev. B* **60** 10565
- [30] O'Hara K E, Gullingsrud J R and Wolfe J P 1999 *Phys. Rev. B* **60** 10872
- [31] Warren J T, O'Hara K E and Wolfe J P 2000 *Phys. Rev. B* **61** 8215
- [32] O'Hara K E and Wolfe J P 2000 *Phys. Rev. B* **62** 12909
- [33] Jang J I and Wolfe J P 2006 *Phys. Rev. B* **74** 045211
- [34] Bulatov A E and Tikhodeev S G 1993 *Phys. Rev. B* **46** 15058
- [35] Tikhodeev S G 1997 *Phys. Rev. Lett.* **78** 3225
Mysyrowicz A, Benson E and Fortin E 1997 *Phys. Rev. Lett.* **78** 3226
- [36] Tikhodeev S G, Kopelevich G A and Gippius N A 1998 *Phys. Status Solidi b* **206** 45
- [37] Fukuzawa T, Kano S S, Gustafson T K and Ogawa T 1990 *Surf. Sci.* **228** 482
- [38] Butov L V 2004 *J. Phys.: Condens. Matter* **16** R1577
- [39] Feldmann J, Peter G, Gobel E O, Dawson P, Moore K, Foxon C and Elliott R J 1987 *Phys. Rev. Lett.* **59** 2337
- [40] Andreani L C, Tassone F and Bassani F 1991 *Solid State Commun.* **77** 641
- [41] Tikhodeev S G 1989 *Solid State Commun.* **72** 1075
- [42] Ivanov A L, Littlewood P B and Haug H 1999 *Phys. Rev. B* **59** 5032
- [43] Butov L V, Ivanov A L, Imamoglu A, Littlewood P B, Shashkin A A, Dolgoplov V T, Campman K L and Gossard A C 2001 *Phys. Rev. Lett.* **86** 5608
- [44] Ivanov A L, Smallwood L E, Hammack A T, Yang S, Butov L V and Gossard A C 2006 *Europhys. Lett.* **73** 920 (Preprint cond-mat/0509097)
- [45] Hammack A T, Griswold M, Butov L V, Smallwood L E, Ivanov A L and Gossard A C 2006 *Phys. Rev. Lett.* **96** 227402 (Preprint cond-mat/0603597)
- [46] Voros Z, Snoke D W, Pfeiffer L and West K 2006 *Phys. Rev. Lett.* **97** 016803
- [47] Butov L V, Mintsev A V, Lozovik Yu E, Campman K L and Gossard A C 2000 *Phys. Rev. B* **62** 1548
- [48] Butov L V, Lai C W, Chemla D S, Lozovik Yu E, Campman K L and Gossard A C 2001 *Phys. Rev. Lett.* **87** 216804
- [49] Lozovik Yu E, Ovchinnikov I V, Volkov S Y, Butov L V and Chemla D S 2002 *Phys. Rev. B* **65** 235304
- [50] Dignam M M and Sipe J E 1991 *Phys. Rev. B* **43** 4084
- [51] Yoshioka D and MacDonald A H 1990 *J. Phys. Soc. Japan* **59** 4211
- [52] Zhu X, Littlewood P B, Hybertsen M and Rice T 1995 *Phys. Rev. Lett.* **74** 1633
- [53] Ivanov A L 2002 *Europhys. Lett.* **59** 586
- [54] Butov L V, Zrenner A, Abstreiter G, Bohm G and Weimann G 1994 *Phys. Rev. Lett.* **73** 304
- [55] Butov L V, Shashkin A A, Dolgoplov V T, Campman K L and Gossard A C 1999 *Phys. Rev. B* **60** 8753
- [56] Ben-Tabou de-Leon S and Laikhtman B 2001 *Phys. Rev. B* **63** 125306
- [57] Butov L V and Filin A I 1998 *Phys. Rev. B* **58** 1980
- [58] Fukuzawa T, Mendez E E and Hong J M 1990 *Phys. Rev. Lett.* **64** 3066
- [59] Kash J A, Zachau M, Mendez E E, Hong J M and Fukuzawa T 1991 *Phys. Rev. Lett.* **66** 2247
- [60] Larionov A V, Timofeev V B, Ni P A, Dubonos S V, Hvam I and Soerensen K 2002 *JETP Lett.* **75** 570
- [61] Dremin A A, Timofeev V B, Larionov A V, Hvam J and Soerensen K 2002 *JETP Lett.* **76** 450
- [62] Butov L V, Gossard A C and Chemla D S 2002 *Nature* **418** 751 (Preprint cond-mat/0204482)
- [63] Snoke D, Denev S, Liu Y, Pfeiffer L and West K 2002 *Nature* **418** 754
- [64] Snoke D 2002 *Science* **298** 1368
- [65] Butov L V, Levitov L S, Mintsev A V, Simons B D, Gossard A C and Chemla D S 2004 *Phys. Rev. Lett.* **92** 117404 (Preprint cond-mat/0308117)
- [66] Rapaport R, Chen G, Snoke D, Simon S H, Pfeiffer L, West K, Liu Y and Denev S 2004 *Phys. Rev. Lett.* **92** 117405 (Preprint cond-mat/0308150)
- [67] Butov L V, Lai C W, Ivanov A L, Gossard A C and Chemla D S 2002 *Nature* **417** 47
- [68] Lai C W, Zoch J, Gossard A C and Chemla D S 2004 *Science* **303** 503
- [69] Szymanska M H and Littlewood P B 2003 *Phys. Rev. B* **67** 193305
- [70] Chemla D S, Miller D A B, Smith P W, Gossard A C and Wiegmann W 1984 *IEEE J. Quantum Electron.* **20** 265
- [71] Yang S, Hammack A T, Fogler M M, Butov L V and Gossard A C 2006 *Phys. Rev. Lett.* **97** 187402 (Preprint cond-mat/0606683)

- [72] Chemla D S and Shah J 2001 *Nature* **411** 549
- [73] Marie X, Le Jeune P, Amand T, Brousseau M, Barrau J, Paillard M and Planel R 1997 *Phys. Rev. Lett.* **79** 3222
- [74] Birkedal D and Shah J 1998 *Phys. Rev. Lett.* **81** 2372
- [75] Langbein W, Hvam J M and Zimmermann R 1999 *Phys. Rev. Lett.* **82** 1040
- [76] Haacke S, Schaer S, Deveaud B and Savona V 2000 *Phys. Rev. B* **61** R5109
- [77] Miller D E, Anglin J R, Abo-Shaer J R, Xu K, Chin J K and Ketterle W 2005 *Phys. Rev. A* **71** 043615
- [78] Östereich Th, Portengen T and Sham L J 1996 *Solid State Commun.* **100** 325
- [79] Laikhtman B 1998 *Europhys. Lett.* **43** 53
- [80] Olaya-Castro A, Rodriguez F J, Quiroga L and Tejedor C 2001 *Phys. Rev. Lett.* **87** 246403
- [81] Zimmermann R 2005 *Solid State Commun.* **134** 43
- [82] Loudon R 2000 *The Quantum Theory of Light* 3rd edn (Oxford: Oxford University Press)
- [83] Scully M O and Zubairy M S 1997 *Quantum Optics* (Cambridge: Cambridge University Press)
- [84] Levitov L S, Simons B D and Butov L V 2005 *Phys. Rev. Lett.* **94** 176404
- [85] Chu S 1998 *Rev. Mod. Phys.* **70** 685
- [86] Cohen-Tannoudji C N 1998 *Rev. Mod. Phys.* **70** 707
- [87] Phillips W D 1998 *Rev. Mod. Phys.* **70** 721
- [88] Ashkin A 2000 *IEEE J. Sel. Items Quantum Electron.* **6** 841
- [89] Hänsch T W and Schawlow A L 1975 *Opt. Commun.* **13** 68
- [90] Anderson M H, Ensher J R, Matthews M R, Wieman C E and Cornell E A 1995 *Science* **269** 198
- [91] Bradley C C, Sackett C A, Tollett J J and Hulet R G 1995 *Phys. Rev. Lett.* **75** 1687
- [92] Davis K B, Mewes M O, Andrews M R, Vandruten N J, Durfee D S, Kurn D M and Ketterle W 1995 *Phys. Rev. Lett.* **75** 3969
- [93] Greiner M, Mandel O, Esslinger T, Hansch T W and Bloch E 2002 *Nature* **415** 39
- [94] Cornell E A and Wieman C E 2002 *Rev. Mod. Phys.* **74** 875
- [95] Ketterle W 2002 *Rev. Mod. Phys.* **74** 1131
- [96] Wolfe J P, Hansen W L, Haller E E, Markiewicz R S, Kittel C and Jeffries C D 1975 *Phys. Rev. Lett.* **34** 1292
- [97] Trauernicht D P, Mysyrowicz A and Wolfe J P 1983 *Phys. Rev. B* **28** 3590
- [98] Kash K, Worlock J M, Sturge M D, Grabbe P, Harbison J P, Scherer A and Lin P S D 1988 *Appl. Phys. Lett.* **53** 782
- [99] Brunner K, Bockelmann U, Abstreiter G, Walther M, Bhöm G, Tränkle G and Weimann G 1992 *Phys. Rev. Lett.* **69** 3216
- [100] Christianen P C M, Piazza F, Lok J G S, Maan J C and van der Vleuten W 1998 *Physica B* **249** 624
- [101] Zimmermann S, Govorov A O, Hansen W, Kotthaus J P, Bichler M and Wegscheider W 1997 *Phys. Rev. B* **56** 13414
- [102] Huber T, Zrenner A, Wegscheider W and Bichler M 1998 *Phys. Status Solidi a* **166** R5
- [103] Hammack A T, Gippius N A, Yang S, Andreev G O, Butov L V, Hanson M and Gossard A C 2005 *Preprint cond-mat/0504045*
- Hammack A T, Gippius N A, Yang S, Andreev G O, Butov L V, Hanson M and Gossard A C 2006 *J. Appl. Phys.* **99** 066104